

Solid Electrolyte Aided Study of the Oxidation of Hydrogen on Copper and Copper Oxide Catalysts

Arthur Balian, George Hatzigiannis, Douglas Eng, and Michael Stoukides¹

Department of Chemical Engineering, Tufts University, Medford, Massachusetts 02155

Received May 17, 1993; revised August 30, 1993

The catalytic oxidation of hydrogen on copper and copper oxide surfaces was studied in a solid electrolyte cell at 250–365°C and 1 atm. The technique of solid electrolyte potentiometry (SEP) was used to monitor the thermodynamic activity of oxygen adsorbed on the catalyst surface during reaction. The oxygen activity value resulted from a steady-state mass balance of oxygen on the catalyst surface and under specific conditions, was several orders of magnitude lower than the gas-phase oxygen partial pressure. The stable phase of the solid was usually CuO and less frequently Cu₂O or metallic Cu. The reaction on reduced (Cu metal) surface exhibited much higher rates than on either oxide, while between the latter two, CuO was the least active surface. The rate-determining step on CuO was the surface reaction between atomically adsorbed hydrogen and oxygen. A kinetic model that quantitatively explains both kinetic and potentiometric measurements in the CuO regime is presented. © 1994 Academic Press, Inc.

INTRODUCTION

The apparently simple recombination of hydrogen and oxygen on metal surfaces is complex from the theoretical viewpoint, and significant kinetic differences among various catalysts have been identified (1–3). Interest in elucidating the mechanism of this reaction has further increased since oscillatory reaction rates were observed on Pt, Ni, and Pd surfaces (4–9). Sustained oscillations have not been reported on copper catalysts during hydrogen oxidation; such phenomena, however, have been observed during propene oxidation on copper (10, 11). The first heterogeneous catalytic reaction in which rate and temperature oscillations were experimentally observed and reported was the decomposition of N₂O over copper oxide (12, 13).

The interpretation of experimental catalytic kinetics of hydrogen oxidation becomes very challenging when, under the conditions of the experiment, the catalyst itself

may undergo oxidation and reduction. In this case, the measured reaction rate may be due to either simply the rate of reduction of the oxide by hydrogen, or the rate of surface recombination of adsorbed hydrogen and oxygen species, or to both. Copper, with two stable oxidation states, Cu^I and Cu^{II}, is a typical example where such difficulties in the interpretation of kinetics have been reported even from the earliest studies (14–18). Part of the disagreement among various earlier and recent works (14–21), however, is also due to the variety of experimental conditions and of catalyst preparation and pretreatment procedures. Depending upon the reaction conditions, the catalyst may be in its reduced metallic form, oxidized to Cu₂O, or oxidized to CuO. Considerable differences between the heats of adsorption on clean and oxidized copper (22) or changes in the rate-determining step upon increasing temperature (23) have been reported.

In the present work, kinetics are combined with potentiometric data in order to study the mechanism of hydrogen oxidation on reduced and oxidized copper surfaces. The technique of solid electrolyte potentiometry (SEP) is used to continuously monitor the thermodynamic activity of oxygen adsorbed on the catalyst surface. This technique, first used in the study of SO₂ oxidation on noble metals (24, 25), has been used in conjunction with kinetic measurements in a large number of metal-catalyzed oxidation reactions (24, 26), including hydrogen oxidation on Ni and on Ag (27–30). More recently, SEP has been applied to metal oxide catalysts (31–34). Hildenbrand and Lintz elegantly showed that SEP can be applied successfully when copper oxides (31) are used as electrodes. Using the same technique, they further studied the partial and complete oxidation of propene to acrolein and carbon dioxide, respectively, on copper oxides and reported on the relationship between reaction rates and phase transformations of the catalyst surface (32, 35). Herein, results of the present work are compared with those of Hildenbrand and Lintz obtained on copper oxides and those obtained during H₂ oxidation on Ni and on Ag (28, 29) using SEP.

¹ To whom correspondence should be addressed at Department of Chemical Engineering, Aristotle University of Thessaloniki, 54006 Thessaloniki, Greece.

EXPERIMENTAL

A detailed description of the experimental apparatus has been provided in previous communications (27–29). The reactor basically consisted of an yttria-stabilized zirconia (solid solution of 8 mole% Y_2O_3 in ZrO_2) tube of 16-mm ID, 19-mm OD and closed at one end. The copper catalyst is placed at the inside bottom of the tube. The concentration of oxygen in the inlet and outlet gaseous streams was monitored by means of a Beckman 755 Paramagnetic Oxygen Analyser. A Fluke 8010A multimeter was used to measure the cell potential. Further details about the experimental apparatus and procedure can be found in Refs. (27–29).

Catalyst Preparation and Characterization

The polycrystalline porous copper film was prepared from metallic copper powder. The powder was mixed with ethylene glycol to form a viscous emulsion. Using a glass rod, droplets of the thick paste were placed at the bottom of the zirconia tube. The tube was placed in a furnace where the catalyst was heated overnight in air at 500°C. Pure oxygen was passed over the catalyst at 400°C for 1 hr. Finally, the catalyst was exposed overnight to a hydrogen stream at 400°C. The catalyst thus produced was a film thin and porous enough that there was substantial length of the air–electrode–electrolyte interline. It was found that reproducible results were obtained if, before each experiment, the catalyst was reduced in a hydrogen stream at 400°C for at least 4 hr. To this end, the above procedure was always followed at the beginning of the experiments and between consecutive runs (36).

Scanning electron micrographs of the copper electrode are shown in Figs. 1, 2, and 3. Figures 1a and 1b show, at $\times 500$ and $\times 5000$ magnification, respectively, a freshly prepared Cu catalyst that was exposed overnight to a hydrogen stream at 350°C. Similarly, Figs. 2a and 2b show a freshly prepared catalyst which, however, has been exposed overnight to air at 350°C and not reduced thereafter. Finally, Figs. 3a and 3b show a Cu electrode that has been exposed overnight to reaction conditions (an H_2 – O_2 mixture with feed mole ratio of $H_2/O_2 = 5$ at 350°C). For an average particle size of 10 microns and for a total mass of metallic copper of 450 mg, the calculated total catalytic surface area was about 200 cm^2 (36).

Silver, instead of copper, was used as reference electrode mainly because silver adheres to the zirconia outside surface much more strongly than copper. The preparation and characterization of the silver electrode has been described in detail in previous communications (29, 37).

Solid Electrolyte Potentiometry

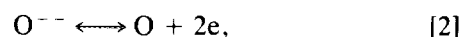
The basic principle and applicability of SEP have also been explained previously (24, 26, 30). SEP utilizes a

stabilized zirconia solid electrolyte cell with one of the electrodes exposed to the reacting mixture and thus serves as a catalyst for the reaction under study. The other electrode is exposed to the air and serves as a reference electrode. The thermodynamic activity of atomic oxygen adsorbed on the catalyst surface is given by the Nernst equation,

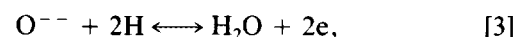
$$a_0 = (0.21)^{1/2} \exp(2FE/RT), \quad [1]$$

where F is the Faraday constant, R is the ideal gas constant, T is the absolute temperature, E is the electromotive force (emf) of the cell, and a_0 is the activity of atomically adsorbed oxygen (29).

The validity of Eq. [1] is based on several assumptions (24, 26), among which the most questionable for the present system, is that atomically adsorbed oxygen is the only species to equilibrate rapidly with oxygen ions at the gas-electrode-electrolyte interline. Although certainly valid for the reference electrode, this assumption may not hold for the catalyst-electrode (24). If, for example, in addition to the O^{--} equilibration with adsorbed oxygen,



a charge transfer reaction with adsorbed hydrogen also takes place at comparable rate,



then a mixed potential is established and the measured emf provides a qualitative and not quantitative measure of surface activities (24, 26). Nevertheless, the emf values attained in the present work (36), were typically between -15 and -300 mv, which is an indication that the assumption in question may be valid (24). Furthermore, Hildenbrand and Lintz (32, 35), assumed the charge transfer reaction [2] dominant and emerged with a reasonable and meaningful interpretation of the potentiometric data. Therefore, in the present study we also first consider that Eq. [1] is valid.

If Eq. [1] holds, the thermodynamic activity of adsorbed atomic oxygen can be continuously monitored during reaction [26]. At the same time the gas-phase oxygen partial pressure above the catalyst surface can be measured independently and the two values can be compared. If thermodynamic equilibrium is established between adsorbed and gaseous oxygen, then $P_{O_2}^{1/2} = a_0$ (26). If, on the other hand, the steady state rates of oxygen adsorption and reaction on the catalyst surface become comparable, then the surface reaction can pull down the surface oxygen activity a_0 to become several orders of magnitude (26, 28, 29) lower than the gas phase activity ($= P_{O_2}^{1/2}$).

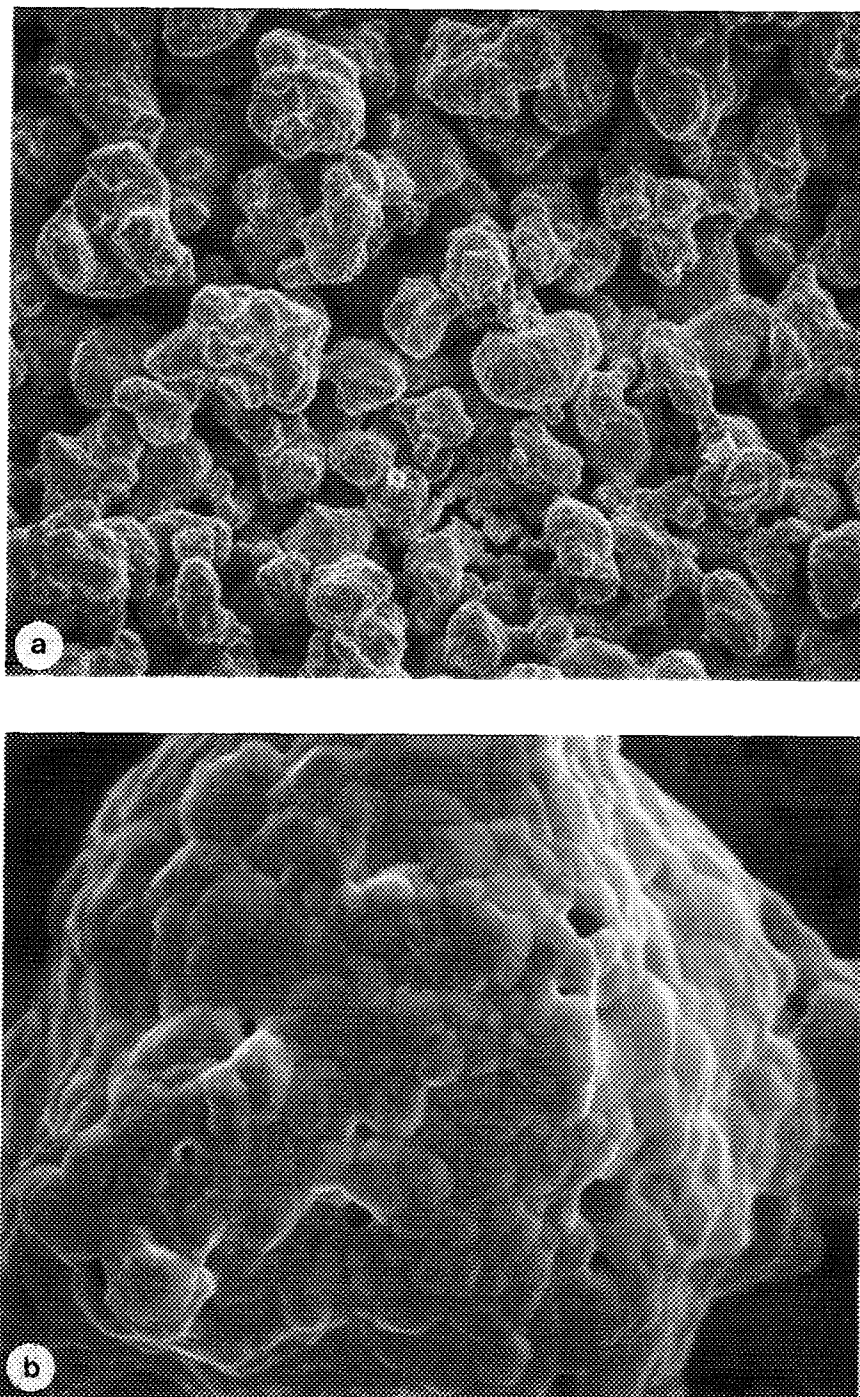


FIG. 1. Scanning electron micrographs of a freshly prepared Cu catalyst that has been exposed overnight to a hydrogen stream at 350°C: (a) at $\times 500$ magnification and (b) at $\times 5000$ magnification.

RESULTS

The reaction rate and the surface oxygen activity behavior was studied at 250–400°C and 1 atm. The hydrogen partial pressure in the reactor exit was var-

ied from 0.005 to 0.38 bar and that of oxygen from 0.0005 to 0.097 bar. Helium was used as diluent and the total volumetric flowrate was varied from 350 to 450 cm³/min. As shown in previous communications (27, 37), the reactor behavior was very close to that

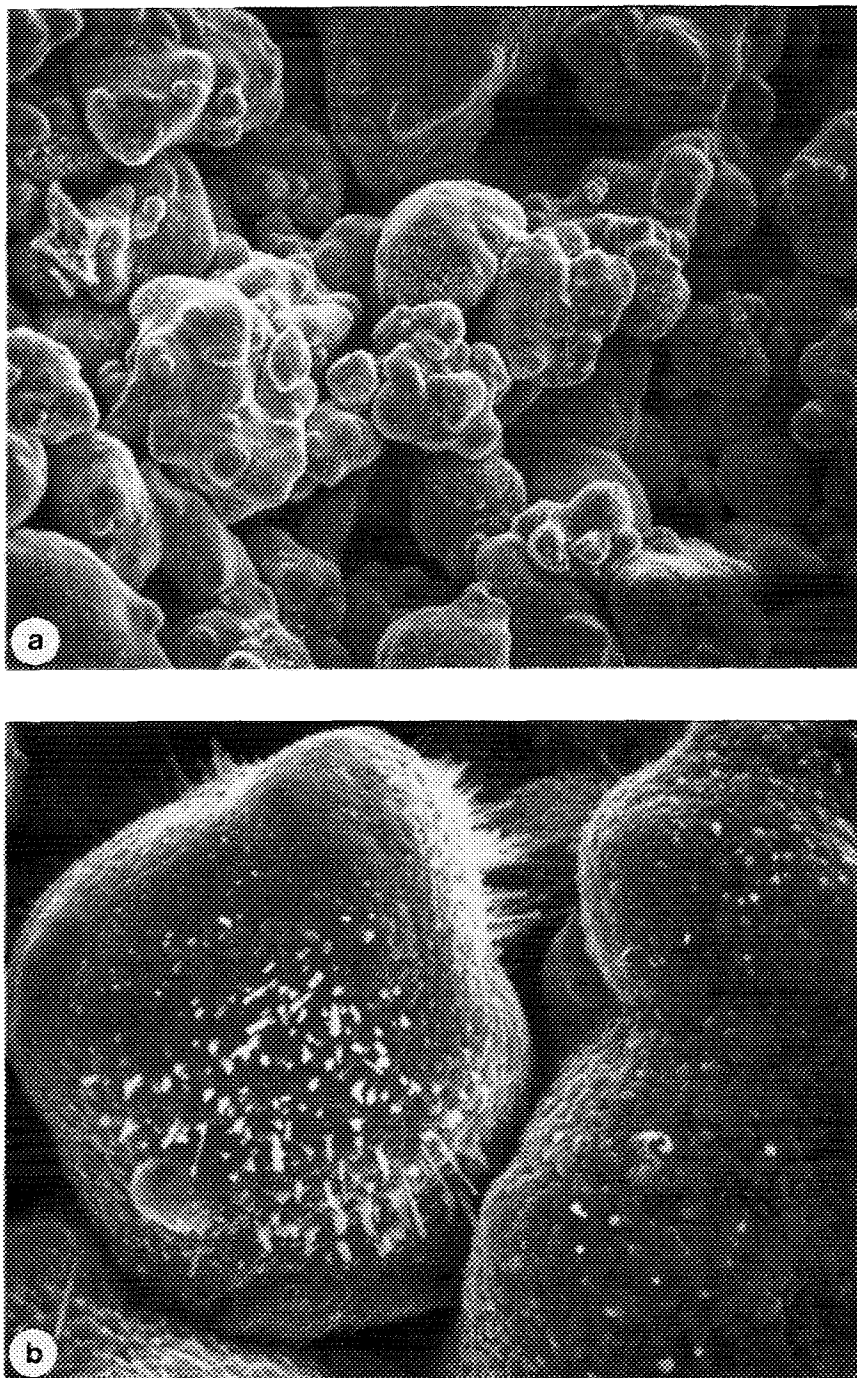


FIG. 2. Scanning electron micrographs of a freshly prepared Cu catalyst that has been exposed overnight to an air stream at 350°C and not reduced thereafter: (a) at $\times 500$ magnification and (b) at $\times 5000$ magnification.

of an ideal CSTR for the above range of volumetric flowrates.

The possibility of noncatalytic (homogeneous in gas phase, reaction on walls, etc.) oxidation of hydrogen was investigated by using a "blank" stabilized zirconia tube, i.e., identical to those used as reactors but without cata-

lyst. Hydrogen and oxygen passed through the blank reactor at partial pressures and temperatures very similar to those during the kinetic studies. Typically, the noncatalytic reaction rate measured was about 1% of the total reaction rate and at the highest temperature examined (365°C), it was 6–8% of the total rate (36). The kinetic

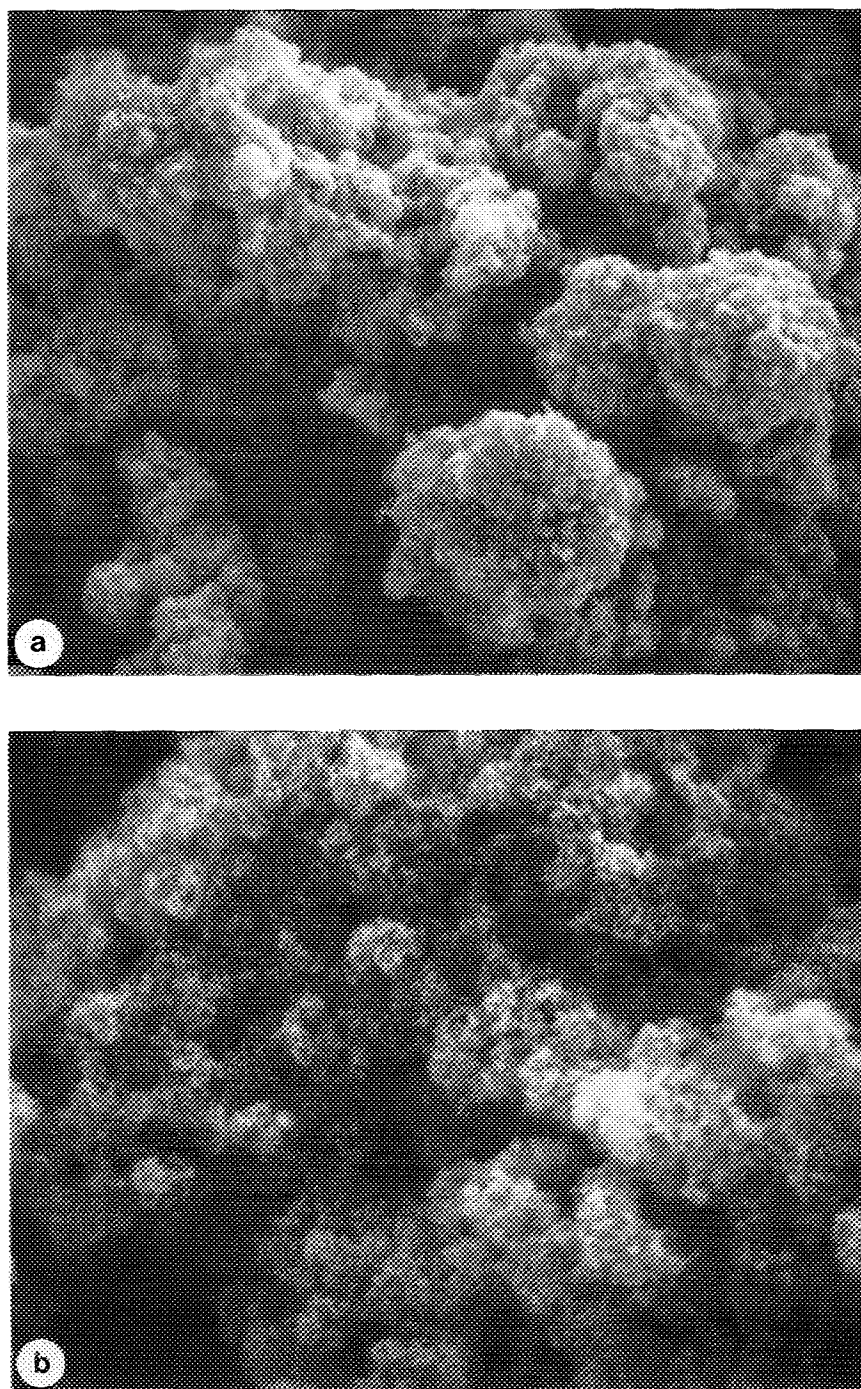


FIG. 3. Scanning electron micrographs of a freshly prepared Cu catalyst that has been exposed overnight to reaction conditions (an H_2-O_2 mixture with feed mole ratio of $H_2/O_2 = 5$ at $350^\circ C$): (a) at $\times 500$ magnification and (b) at $\times 5000$ magnification.

results presented have been corrected by subtracting the homogeneous effect. External and internal diffusion limitations were insignificant as confirmed by varying appropriately the volumetric flowrate and the thickness of the catalyst film. There were no signs of deactivation of the

copper catalyst for at least 3–4 weeks of operation as long as the temperature remained between 200 and $400^\circ C$ (36).

All the results that follow correspond to steady states. We considered that a steady state was reached when there was no more than 3% change in the outlet P_{O_2} and a_0

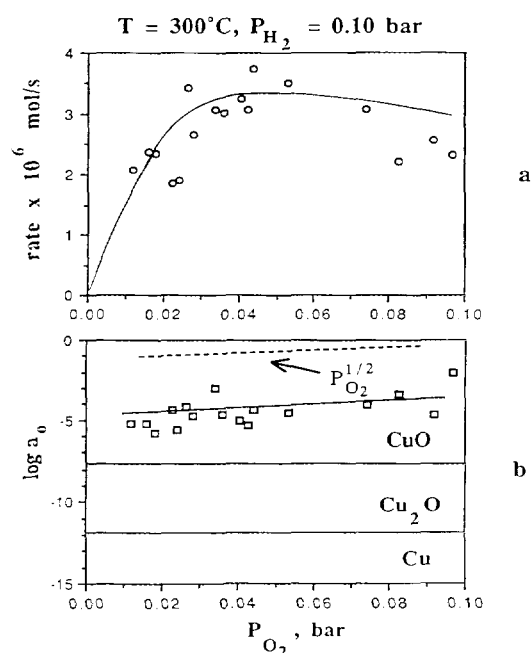


FIG. 4. Dependence of reaction rate and surface oxygen activity on the outlet partial pressure of oxygen. $T = 300^{\circ}\text{C}$ and $P_{\text{H}_2} = 0.10$ bar.

values over 1 hour. Typically, such steady states were attained within one to two hours after a new gaseous composition was fed in the reactor following the catalyst reduction by hydrogen at 400°C for 4 hr. Since more than one cell were used to obtain the present results, a "control test" was done with each of the catalysts at a given temperature and gas composition (300°C , $P_{\text{H}_2} = 0.10$ bar, $P_{\text{O}_2} = 0.025$ bar). Then, the ratio of surface areas of two catalysts was taken as equal to the ratio of reaction rates that the catalysts gave at the control test (36). Consequently, since the preparation procedure was exactly the same for all catalysts, we assumed that for any two catalyst films, the surface area ratio was equal to the mass ratio. The results presented below were based on a 450-mg catalyst.

The reaction rate was calculated from the oxygen mass balance,

$$r = 2G(X_{\text{O}_2,\text{in}} - X_{\text{O}_2,\text{out}}), \quad [4]$$

where r is the reaction rate in moles of H_2O per second, G is the total molar flowrate, and $X_{\text{O}_2,\text{in}}$ and $X_{\text{O}_2,\text{out}}$ are the mole fractions of oxygen in the feed and in the outlet, respectively.

Figure 4 shows the dependence of the reaction rate and the surface oxygen activity on the partial pressure of oxygen in the reactor at 300°C . The outlet partial pressure of hydrogen was maintained at 0.10 bar. As seen in Fig.

4a, the reaction rate initially increases sharply to reach a maximum and then decreases following negative-order kinetics. The corresponding a_0 values shown in Fig. 4b, vary from 10^{-6} to 10^{-2} and increase with increasing P_{O_2} . The dotted line above the a_0 data corresponds to the gas-phase $P_{\text{O}_2}^{1/2}$ values in the reactor. If thermodynamic equilibrium were established between adsorbed and gaseous oxygen, the dotted line and the potentiometric data would coincide. Clearly, the a_0 values are lower than the $P_{\text{O}_2}^{1/2}$ values. The continuous horizontal lines correspond to the thermodynamic stability limits of the three solid phases of the copper–oxygen system (Cu, Cu_2O , and CuO) at this temperature. They have been calculated from literature-reported values (36, 38) of the free energy of formation of these compounds and they were confirmed by comparing them to those shown in Hildenbrand and Lintz (31, 32). The bottom horizontal line represents the a_0 value below which only metallic copper is thermodynamically stable. Similarly, the upper continuous horizontal line represents the a_0 value above which only the CuO is thermodynamically stable. The Cu_2O phase is stable between the two parallel lines i.e., for a_0 values between 9.1×10^{-13} and 1.58×10^{-8} . Each continuous straight line physically represents a unique a_0 value at which two solid phases ($\text{Cu}-\text{Cu}_2\text{O}$ and $\text{Cu}_2\text{O}-\text{CuO}$ for the bottom and upper line, respectively) are thermodynamically allowed to coexist at that temperature. It can be clearly seen in Fig. 4b that all the experimentally obtained values of a_0 fall in the regime in which the thermodynamically stable phase is CuO . Finally, the solid lines through the data points correspond to the predictions of the model as explained in the Discussion section.

Similar curves at different P_{H_2} and P_{O_2} levels were obtained at temperatures between 250 and 350°C . Due to safety considerations, the region of oxygen–hydrogen compositions was limited by the lower and upper explosion limits of hydrogen in oxygen (27). Figures 5 and 6 contain rate and oxygen activity data obtained at 250°C . In Fig. 5, oxygen is varied for constant $P_{\text{H}_2} = 0.1$ bar. In Fig. 6, hydrogen is varied for constant $P_{\text{O}_2} = 0.05$ bar. It can be seen again, that all the data fall in the a_0 regime where CuO is the thermodynamically stable solid phase.

In Fig. 7, r and a_0 are plotted vs P_{H_2} at 300°C and with constant outlet $P_{\text{O}_2} = 0.05$ bar. The reaction rate increases moderately with hydrogen up to a P_{H_2} value of about 0.11 bar above which a sharp rate increase is observed (Fig. 7a). The surface oxygen activity decreases with increasing P_{H_2} , intersects the $\text{CuO}-\text{Cu}_2\text{O}$ stability line and continues decreasing (Fig. 7b). Noteworthy is that the inflexion point (dotted vertical line) in the reaction rate data corresponds to the critical oxygen activity value at which the surface changes from CuO to the Cu_2O phase. As in Fig. 4, the dotted, solid, and continuous horizontal lines corre-

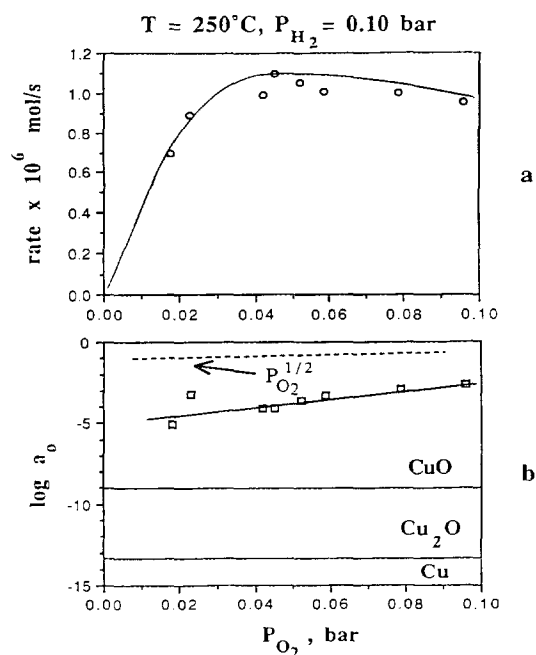


FIG. 5. Dependence of reaction rate and surface oxygen activity on the outlet partial pressure of oxygen. $T = 250^\circ\text{C}$ and $P_{\text{H}_2} = 0.10$ bar.

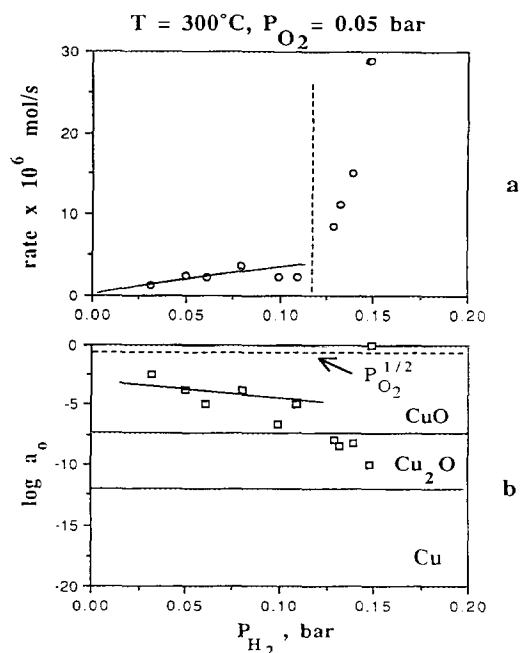


FIG. 7. Dependence of reaction rate and surface oxygen activity on the outlet partial pressure of hydrogen. $T = 300^\circ\text{C}$ and $P_{\text{O}_2} = 0.05$ bar.

spond to $P_{\text{O}_2}^{1/2}$, model predictions, and oxide stability limits, respectively.

Results obtained at 350°C with P_{O_2} held at 0.05 bar and varying the outlet P_{H_2} are shown in Fig. 8. At this temperature, the a_0 data can be also found in both the CuO and

the Cu_2O regimes. Again, the Cu_2O surface seems to be catalytically more active than CuO.

As shown in Figs. 4–8, the experimentally obtained a_0 values were usually in the range within which the stable solid phase is CuO. Less often, and generally at high

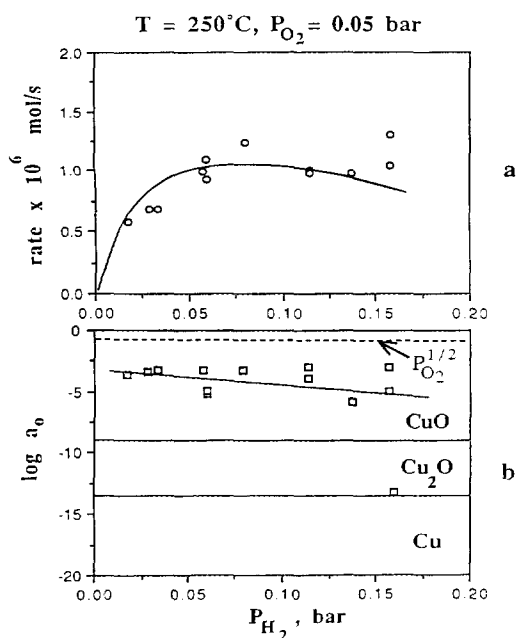


FIG. 6. Dependence of reaction rate and surface oxygen activity on the outlet partial pressure of hydrogen. $T = 250^\circ\text{C}$ and $P_{\text{O}_2} = 0.05$ bar.

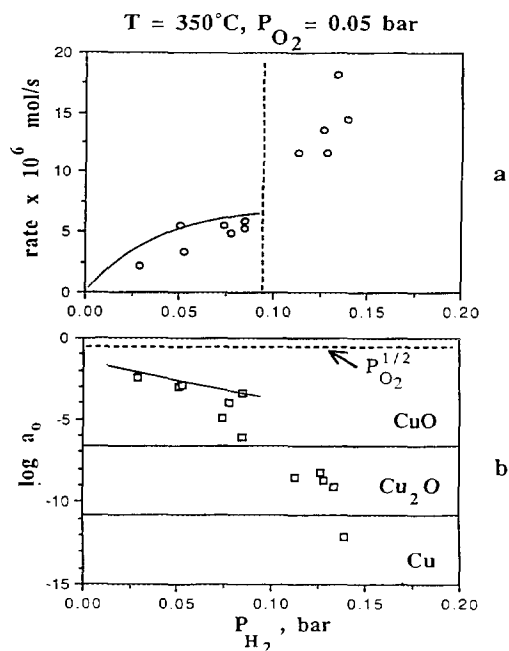


FIG. 8. Dependence of reaction rate and surface oxygen activity on the outlet partial pressure of hydrogen. $T = 350^\circ\text{C}$ and $P_{\text{O}_2} = 0.05$ bar.

P_{H_2} , a_0 values corresponding to Cu_2O were also observed. To get into the metallic Cu range, the hydrogen/oxygen ratio had to be very high ($P_{H_2}/P_{O_2} > 25$ at $365^\circ C$ and even higher at lower temperatures). This can be seen in Fig. 9, where kinetic and SEP data are presented for $365^\circ C$. The outlet P_{O_2} was allowed to vary. Due to experimental difficulties, the outlet P_{H_2} was only approximately constant (varied from 0.078 to 0.106 bar). As shown in Fig. 9b, the a_0 values attained were between 2.8×10^{-13} and 2×10^{-5} , while the critical a_0 values for phase transformations at that temperature are 4×10^{-11} and 3×10^{-7} for the Cu/ Cu_2O and the Cu_2O /CuO systems, respectively (36).

DISCUSSION

The kinetics of the copper-catalyzed oxidation of hydrogen has been a stimulating problem for a long time. Pease and Taylor studied the reaction at oxygen contents between 0 and 5% and at temperatures of 100 – $200^\circ C$ (15, 39). They suggested that in addition to the reaction between adsorbed hydrogen and oxygen, water is formed from the reduction of the oxide (15). When O_2 was shut off and only H_2 was fed over the oxidized surface, the oxide was reduced at a rate greater than that of H_2O formation in presence of gaseous oxygen (15, 39). Larson and Smith studied the reaction at 34 – $130^\circ C$ and suggested that two reactions occurred simultaneously on the catalyst surface, reduction of the oxide and the union of adsorbed H and O, the latter being probably faster (16). Wilkins and Bastow tried to correlate the rates of oxidation and reduction of Cu to the rate of H_2O formation. Their results suggested that surface reaction was taking place in addition to the oxidation–reduction process (17).

Reviewing the results of previous investigators, Van Cleave and Rideal pointed out the difficulty in determining which oxide of copper existed under reaction conditions (18). The above authors also studied the reaction at 170 – $360^\circ C$ and concluded that, depending on the conditions, there are three processes that control the rate of water formation:

(a) for copper reduced in H_2 , the rate determining step is the activated diffusion of hydrogen in copper ($E_a = 13$ Kcal/mole). Both surface reaction and oxide formation occur during that process.

(b) At slightly oxidized surface, water formation via adsorbed species is coupled with oxide reduction, the oxide being primarily Cu_2O . The apparent activation energy for the reaction is about 6 Kcal/mole.

(c) Upon prolonged exposure to H_2 – O_2 mixture, CuO is the abundant phase and it acts as a true catalyst, i.e., H_2O is formed by the reaction of oxygen and hydrogen adsorbed on the CuO surface. The apparent activation energy for the reaction is 9 Kcal/mole (18).

More recently, Domen et al used XPS to study the

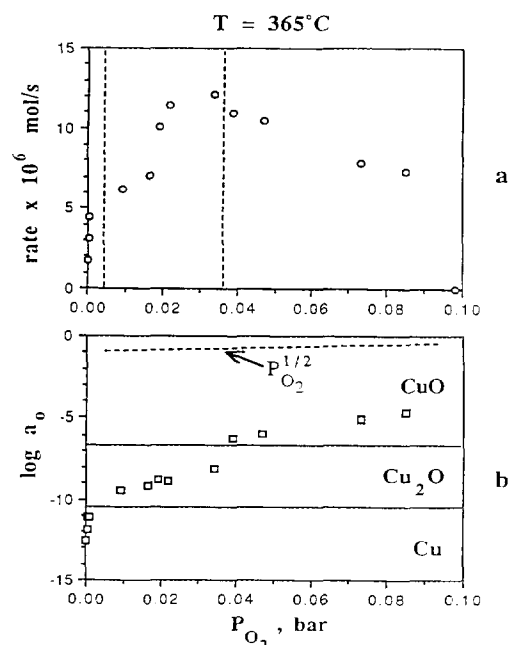


FIG. 9. Dependence of reaction rate and surface oxygen activity on the outlet partial pressure of oxygen. $T = 250^\circ C$ and $P_{H_2} = 0.078$ – 0.106 bar.

H_2 – O_2 interaction on copper at 120 – $150^\circ C$ (21). Water was found to be formed by adsorbed rather than lattice oxygen and the reaction proceeded primarily on a Cu_2O surface. Upon oxidation in absence of H_2 , CuO was formed and reduced metallic Cu appeared only at very low O_2/H_2 ratios. The reaction order with respect to hydrogen was oxygen-dependent and varied from 0.6 (low P_{O_2} region) to 1.0 (high P_{O_2} region).

Here, the reaction of hydrogen and oxygen on copper is examined in view of the kinetic and potentiometric information that has become available. A kinetic model proposed should explain not only the kinetics but also the SEP measurements. Nevertheless, the analysis presented below is limited to the data of the region where a_0 values exceed values corresponding to the Cu_2O /CuO stability limit (CuO region). There are two reasons for that:

(a) In the CuO region, in agreement with previous works (18), we can consider that the measured H_2O formation rates are due to catalytic reaction between adsorbed species. In the other two regions, oxide reduction and catalytic reaction are probably coupled.

(b) The a_0 values in the CuO region were large enough (emf typically between -40 and -180 mV) to safely assume that Eq. [1] is valid. In the other two regions, however, and especially in the metallic Cu region, the emf values were sometimes so low that the validity of Eq. [1] may become questionable.

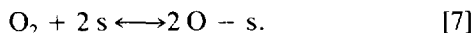
Considering the reaction on CuO only, we can first assume dissociative adsorption of hydrogen,



and also assume that this step is close to equilibrium so that

$$\theta_{\text{H}} = K_{\text{H}} \theta_{\text{s}} P_{\text{H}_2}^{1/2}, \quad [6]$$

where θ_{H} and θ_{s} stand for fractional coverages of hydrogen and empty sites, respectively, and K_{H} is the adsorption coefficient of atomic hydrogen. Similarly, we can consider dissociative adsorption of oxygen:



The fractional coverage of atomic oxygen is related to the surface oxygen activity a_0 via the equation

$$\theta_0 = K_0 \theta_{\text{s}} a_0, \quad [8]$$

where K_0 is the adsorption coefficient of atomic oxygen. Note that the above equation is valid irrespective of whether equilibrium is established between adsorbed and gaseous oxygen or not (29). Assuming that the slow step is the interaction between adsorbed oxygen and hydrogen, the reaction rate r can be written as

$$r = k_{\text{R}} \theta_0 \theta_{\text{H}}. \quad [9]$$

Using Eqs. [6] and [8] and assuming that $\theta_0 + \theta_{\text{H}} + \theta_{\text{s}} = 1$, the above rate expression becomes

$$r = k_{\text{R}} k_0 a_0 K_{\text{H}} P_{\text{H}_2}^{1/2} / (1 + K_0 a_0 + K_{\text{H}} P_{\text{H}_2}^{1/2})^2 \quad [10]$$

In addition to Eq. [10], a steady-state balance for adsorbed oxygen gives

$$k_1 P_{\text{O}_2} \theta_{\text{s}}^2 - k_{-1} \theta_0^2 - r/2 = 0, \quad [11]$$

where the first and second left-hand terms correspond to O_2 adsorption and desorption, respectively, and the last one accounts for half the rate of consumption of atomic oxygen. Using equations [6] and [8] and dividing by $k_1 \theta_{\text{s}}^2$ all terms of equation [11], we obtain:

$$P_{\text{O}_2} - a_0^2 = r/2k_1 \theta_{\text{s}}^2 = r(1 + K_0 a_0 + K_{\text{H}} P_{\text{H}_2}^{1/2})^2 / 2k_1. \quad [12]$$

Equations [10] and [12] relate the experimentally measured a_0 , r , P_{O_2} and P_{H_2} with the temperature-dependent constants K_0 , K_{H} , k_1 , and k_{R} . The values for the constants that could best fit the data at 250–350°C (36) were found to be

$$k_1 = 0.0011 \exp(-460/T) \text{ mole O}_2/\text{s} \quad [13]$$

$$K_0 = 1.67 \times 10^{-3} \exp(8700/T) \text{ bar}^{-1/2} \quad [14]$$

$$K_{\text{H}} = 2.15 \times 10^{-3} \exp(4300/T) \text{ bar}^{-1/2} \quad [15]$$

$$k_{\text{R}} = 32.9 \exp(-8100/T) \text{ mole H}_2\text{O/s.} \quad [16]$$

The values of the kinetic and thermodynamic constants justify reasonably well the physical significance attributed to them. For example, k_1 , the adsorption rate constant for O_2 , has a temperature dependence of a little less than one kcal/mole, i.e., the adsorption is only slightly activated. Also, the heat of adsorption of atomic oxygen is about 17.5 kcal/mole, almost twice that of atomically adsorbed hydrogen. In Figs. 4–8, the dotted lines represent the model predictions for a_0 and r . Needless to say, the above kinetic model is not the only one to explain the present kinetic and potentiometric results. Several previous works suggested the formation of hydroxyl species on the surface. The formation of OH was not explicitly written down in the present model because there was no direct evidence of its existence on the surface by SEP or any of the techniques used in the present work. Nevertheless, a model that involves OH formation could explain the experimental findings equally well.

As mentioned previously, no attempt was made to come up with equations equivalent to Eqs. [10] and [12] for the Cu_2O and Cu regions. A rough comparison, however, of catalytic activities in the three regions can be done using the data of Fig. 9. Assuming first-order kinetics for both H_2 and O_2 , the turnover rates for the CuO, Cu_2O , and Cu surfaces are proportional to 1, 2.5, and 24, respectively, which implies that metallic copper is much more active than either oxide. The problem, of course, is that when the catalyst is exposed to high P_{O_2} , the surface can no longer remain in the metallic form, especially in a CSTR type of reactor where the outlet concentrations cannot differ from those over the catalyst. Nevertheless, in a hydrogen fueled solid oxide fuel cell where oxygen is supplied through the solid wall as O^{2-} , the catalyst-electrode may more easily maintain its reduced form and thus high reaction rates may be achieved.

The present results verify earlier works which pointed out that in open systems the oxygen content of the catalyst is not necessarily the thermodynamically predicted but is rather kinetically determined (40, 41). If thermodynamic equilibrium were established between gaseous and adsorbed oxygen, then $P_{\text{O}_2}^{1/2}$ would be equal to a_0 , where the dotted $P_{\text{O}_2}^{1/2}$ lines in Figs. 4–9 would coincide with the a_0 data. Consequently, CuO would be the thermodynamically stable phase for all the data of the above figures because the gas phase value of P_{O_2} never was below the 10^{-6} bar (or equivalently, $P_{\text{O}_2}^{1/2} > 10^{-3} \text{ bar}^{1/2}$). Depending on the temperature and the gas composition, however,

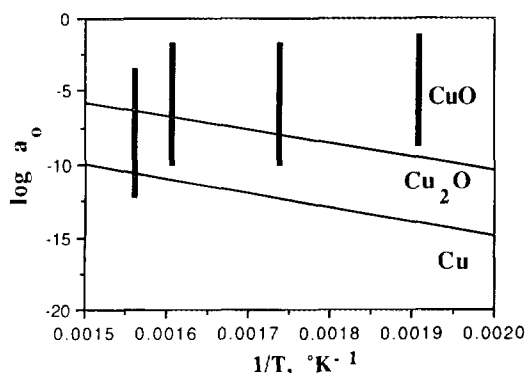


FIG. 10. Comparison of stability limits for CuO and Cu₂O formation with oxygen activity values obtained experimentally.

the surface oxygen activity a_0 could become so low that Cu₂O or even Cu would become the thermodynamically stable phase as seen in Fig. 10, where $\log a_0$ is plotted vs $1/T$. The upper and bottom continuous straight lines correspond to the stability limits of CuO and Cu₂O, respectively. The vertical bars correspond to the range of values of a_0 that were experimentally attained in this study (36). How low a_0 can get is a matter of steady state mass balance of oxygen on the catalyst as described by Eqs. [11] or [12]. Equation [12] shows that the deviation of a_0^2 from P_{O_2} is a function of the magnitude of the reaction rate r . If $r = 0$, then $a_0 = P_{O_2}^{1/2}$. Typically, the a_0 values were 1 to 3 orders of magnitude lower than the $P_{O_2}^{1/2}$ values.

SEP has been used in the studies of hydrogen oxidation on Ni and Ag. On nickel catalysts the deviation of a_0 from $P_{O_2}^{1/2}$ was from 3 to as much as 10 orders of magnitude (27, 28). On silver, $P_{O_2}^{1/2}$ exceeded a_0 by a factor of 5–15 only (29). Clearly, in the case of Ag, reaction on the surface was rate determining and only occasionally oxygen adsorption and surface reaction attained comparable rates. On Ni, on the other hand, the reaction was almost always limited by the adsorption of oxygen and therefore a mass balance of oxygen on the catalyst gave very low values for a_0 . This can be also seen in Eq. [11], where as “ $r/2$ ” approaches “ $k_1 P_{O_2} \theta_s^2$,” the term “ $k_1 \theta_0^2$,” (which is proportional to a_0^2), approaches zero.

Phase transitions and hysteresis phenomena were observed on copper oxide catalysts during the oxidation of propene (42, 43), and later, thermochemical oscillations during the study of the same reaction were also reported (10, 11). The phase changes associated with the observed oscillations were identified by X-ray analysis (11). In agreement with previous studies (32, 38), it was found that acrolein formation was favored on Cu₂O, while CuO favored the formation of carbon dioxide (11). Due to the much more exothermic reaction of CO₂ formation than that of acrolein, a thermochemical cycle was created over

the catalyst surface shifting periodically from one copper oxide to the other (11).

Hildebrand and Lintz (32, 35) used SEP during the study of propene oxidation on copper oxides and were able to determine the solid phase that was thermodynamically stable. They more easily obtained data in the Cu and Cu₂O regimes than in the present study because (a) their reaction was studied at higher temperatures (420–510°C) where the stability limits for either oxide are shifted to higher a_0 values and (b) the rate of consumption of surface oxygen (including CO₂ formation) in their case, was about one order of magnitude higher than the rates observed in the present study.

Unlike those studies with propene oxidation, oscillatory phenomena were not observed in this work. There was no systematic search in the Cu/Cu₂O transition region. Nevertheless, enough data were obtained in the temperature and gas composition regime where the Cu₂O/CuO transition takes place. This is consistent with the interpretation of the oscillatory behavior provided by Amariglio *et al.* (11). Water is the only product from the oxidation of hydrogen either on Cu₂O or on CuO. Therefore the large difference in reaction enthalpies between carbon dioxide and acrolein formation does not apply here. The present work verifies that a phase change on the catalyst surface is not sufficient to produce sustained oscillations. A number of additional conditions need to be met as well.

SUMMARY

Solid electrolyte potentiometry was a useful tool in the study of hydrogen oxidation on reduced and oxidized copper catalysts. Using this technique, it was possible to monitor the thermodynamic activity of oxygen adsorbed on the catalyst surface during reaction. Under certain conditions, the activity of adsorbed oxygen could become much lower than the partial pressure of gaseous oxygen so that the stable phase of the catalyst was no longer CuO but Cu₂O and occasionally metallic Cu. The reaction on CuO followed Langmuir–Hinselwood kinetics with the adsorption of atomic oxygen being much stronger than that of hydrogen. The reaction on cuprous oxide (Cu₂O) was faster than on CuO, while reduced copper was by far the best of the three as a catalyst for this reaction. Nevertheless, high temperatures and high hydrogen/oxygen ratios were needed to maintain the catalyst in its reduced form. Mainly for this reason, the reaction was not studied in the Cu/Cu₂O transition regime as extensively as in the Cu₂O/CuO region which was much more easily attainable. Isothermal oscillatory phenomena were not observed in any of the regimes studied. Within a finite period of time, stable steady states were always obtained.

ACKNOWLEDGMENTS

We gratefully acknowledge the National Science Foundation and the Department of Energy for support of this work under Grants CBT-8815927 and DE-89-CE90048, respectively. Also, one of the authors (M.S.), kindly acknowledges partial support by the EEC through the JOULE II Non-Nuclear Energy Research Program.

REFERENCES

- Norton, P. R., in "The Chemical Physics of Solid Surfaces and Heterogeneous Catalysis" (D. A. King and D. P. Woodruff, Eds.), Vol. 4. Elsevier, New York, 1982.
- Haruta, M., Souma, Y., and Sano, H., in "Proceedings, 3rd World Hydrogen Energy Conference," Vol. 2, 1980.
- Bond, G. C., "Catalysis by Metals," Academic Press, London, 1962.
- Kurtanek, Z., Sheintuch, M., and Luss, D., *J. Catal.* **66**, 11 (1980).
- Belyaev, V. D., Slinko, M. M., Timoshenko, V. I., and Slinko, M. G., *Kinet. Katal.* **14**, 810 (1973).
- Rajagopalan, K., Sheintuch, M., and Luss, D., *Chem. Eng. Commun.* **7**, 335 (1980).
- Zuniga, J. E., and Luss, D., *J. Catal.* **53**, 312 (1978).
- Saidi, G., and Tsotsis, T., *Surf. Sci.* **161**, L591 (1985).
- Tsai, P. K., and Maple, M. B., *J. Catal.* **101**, 142 (1986).
- Amariglio, A., Benali, O., and Amariglio, H., *C.R. Acad. Sci. Paris Ser. II* **307**, 897 (1988).
- Amariglio, A., Benali, O., and Amariglio, H., *J. Catal.* **118**, 164 (1989).
- Hugo, P., "Chem. React. Eng. Proc.: 4th Europ. Symp." p. 459. Pergamon, Oxford, 1971.
- Sheintuch, M., and Schmitz, R., *Catal. Rev.-Sci. Eng.* **15**(1), 107 (1977).
- Bone, W. A., and Wheeler, R. V., *Philos. Trans.* **206A**, 1 (1906).
- Pease, R. N., and Taylor, H. S., *J. Am. Chem. Soc.* **44**, 1637 (1922).
- Larson, A. T., and Smith, F. E., *J. Am. Chem. Soc.* **47**, 346 (1925).
- Wilkins, F. J., and Bastow, S. H., *J. Chem. Soc.*, 1525 (1931).
- Van Cleave, A. B., and Rideal, E. K., *Trans. Faraday Soc.* **33**, 635 (1937).
- Ostrovsky, V. E., and Dobrovolsky, N. N., in "Proceedings, 4th International Congress on Catalysis, Moscow, 1968" (B. A. Kazansky, Ed.), pp. 823-840. Adler, New York, 1968.
- Davydova, L. P., Bulgakov, N. N., Aleksandrov, V. Yu., and Popovskii, V. V., *Kinet. Katal.* **21**, 988 (1980).
- Domen, K., Naito, S., Soma, M., Onishi, T., and Tamaru, K., *J. Chem. Soc. Faraday Trans. 1* **78**, 845 (1982).
- Dell, R. M., Stone, F. C., and Tiley, P. F., *Trans. Faraday Soc.* **49**, 195 (1953).
- Hayden, B. E., and Lamont, C. L. A., *J. Phys.: Condens. Matter* **1**, SB33 (1989).
- Vayenas, C. G., Bebelis, S., Yentekakis, I. V., and Lintz, H. G., *Catal. Today* **11**, 303 (1992).
- Vayenas, C. G., and Saltsburg, H. M., *J. Catal.* **57**, 296 (1979).
- Stoukides, M., *Ind. Eng. Chem. Res.* **27**, 1745 (1988).
- Saranteas, C., and Stoukides, M., *J. Catal.* **93**, 417 (1985).
- Eng, D., Stoukides, M., and McNally, T., *J. Catal.* **106**, 342 (1987).
- Hillary, A., and Stoukides, M., *J. Catal.* **113**, 295 (1988).
- Vayenas, C. G., *Solid State Ionics*, **28-30**, 1521 (1988).
- Hildenbrand, H.-H., and Lintz, H.-G., *Appl. Catal.* **49**, L1 (1989).
- Hildenbrand, H.-H., and Lintz, H.-G., *Appl. Catal.* **65**, 241 (1990).
- Gellings, P. J., Koopmans, H. S. A., and Burggraaf, A. J., *Appl. Catal.* **39**, 1 (1988).
- Breckner, E. M., Sundaresan, S., and Benziger, J. B., *Appl. Catal.* **30**, 277 (1987).
- Hildenbrand, H. H., and Lintz, H.-G., *Catal. Today* **9**, 153 (1991).
- Balian, A., M.S. Thesis, Tufts University, 1992.
- Stoukides, M., and Vayenas, C. G., *J. Catal.* **64**, 18 (1980).
- Barin, I., and Knacke, O., in "Thermochemical Properties of Inorganic Substances." Springer-Verlag, Berlin/Dusseldorf, 1973.
- Pease, R. N., and Taylor, H. S., *J. Am. Chem. Soc.* **43**, 2179 (1921).
- Wagner, C., *Ber. Bunsenges. Phys. Chem.* **74**, 401 (1970).
- Riekert, L., *Ber. Bunsenges. Phys. Chem.* **85**, 297 (1981).
- Greger, M., Ihme, B., Kotter, M., and Riekert, L., *Ber. Bunsenges. Phys. Chem.* **88**, 427 (1984).
- Greger, M., and Riekert, L., *Ber. Bunsenges. Phys. Chem.* **91**, 1007 (1987).